Hybridization of PNA to Structured DNA Targets: Quadruplex Invasion and the Overhang Effect

Bhaskar Datta and Bruce A. Armitage*

Contribution from the Department of Chemistry, Carnegie Mellon University, 4400 Fifth Avenue, Pittsburgh, Pennsylvania 15213-3890

Received May 16, 2001

Abstract: Peptide nucleic acid (PNA) probes have been synthesized and targeted to quadruplex DNA. UV−vis and CD spectroscopy reveal that the quadruplex structure of the thrombin binding aptamer (TBA) is disrupted at 37 °C by a short PNA probe. The corresponding DNA probe fails to bind to the stable secondary structure at this temperature. Thermal denaturation experiments indicate surprisingly high thermal and thermodynamic stabilities for the PNA−TBA hybrid. Our results point to the nonbonded nucleobase overhangs on the DNA as being responsible for this stability. This "overhang effect" is found for two different PNA−DNA sequences and a variety of different overhang lengths and sequences. The stabilization offered by the overhangs assists the PNA in overcoming the stable secondary structure of the DNA target, an effect which may be significant in the targeting of biological nucleic acids, which will always be much longer than the PNA probe. The ability of PNA to invade a structured DNA target expands its potential utility as an antigene agent or hybridization probe.

Introduction

The use of Watson−Crick base pairing to target specific sequences of DNA and RNA forms the basis for a variety of therapeutic and diagnostic methods. For example, antisense oligonucleotides can bind to complementary messenger RNA sequences and prevent translation of the mRNA into protein. Peptide nucleic acid (PNA) represents a promising class of synthetic antisense DNA analogues in which the entire sugar−phosphate backbone is replaced by a pseudopeptide.[1−6] PNAs combine high affinity and sequence specificity for complementary DNA and RNA[7] with high chemical stability to protease and nuclease enzymes,[8] favorable properties for antisense/antigene agents and hybridization probes. Homopyrimidine PNAs can bind to complementary homopurine target sites in double-stranded (ds) DNA by the mechanism of strand invasion.[9] Mixed sequence PNAs can also bind to ds DNA using a double strand invasion mechanism where both DNA strands are targeted.[10] Strand invasion by mixed base PNAs and PNA−peptide chimera has also been reported.[11,12] Such invasion complexes can impose a structural impediment to RNA polymerase[13] and thus have potential as antigene agents.[14]

The PNA antisense effect is based on the steric blocking of either RNA processing or translation. Both duplex- (mixed sequence) and triplex-forming (pyrimidine-rich) PNAs have been found to inhibit translation at targets overlapping the AUG start codon.[15] Another study demonstrated the effect of two bis-PNAs, targeted against the homopurine stretches in rRNA, inhibiting the ribosome function in a cell-free system and also showing bactericidal activity.[16−18] PNA probes have also been used for telomerase inhibition. Telomerase is a ribonucleoprotein that adds repeating units of d(TTAGGG) to the ends of human chromosomes,[19] and its activity is associated, though not always, with tumorigenesis.[20] Targets for telomerase inhibition include an RNA template and specialized structures that may be formed by newly synthesized telomeric DNA.[21] There are numerous reports of PNA being targeted to the RNA component of

* To whom correspondence should be addressed. E-mail: army@cyrus.andrew.cmu.edu.

(1) Nielsen, P. E.; Egholm, M.; Berg, R. H.; Buchardt, O. *Science* **1991**, *254*, 1498−1500.
(2) Nielsen, P. E. *Pure Appl. Chem.* **1998**, *70*, 105−110.
(3) Uhlmann, E.; Peyman, A.; Breipohl, G.; Will, D. W. *Angew. Chem., Int. Ed.* **1998**, *37*, 2796−2823.
(4) Corey, D. R. *Trends Biotechnol.* **1997**, *15*, 224−229.
(5) Nielsen, P. E.; Haaima, G. *Chem. Soc. Rev.* **1997**, *26*, 73−78.
(6) Erikkson, M.; Nielsen, P. E. *Q. Rev. Biophys.* **1996**, *29*, 369−394.
(7) Egholm, M.; Buchardt, O.; Christensen, L.; Behrens, C.; Freier, S. M.; Driver, D. A.; Berg, R. H.; Kim, S. K.; Nordén, B.; Nielsen, P. E. *Nature* **1993**, *365*, 566−568.
(8) Demidov, V. V.; Potaman, V. N.; Frank-Kamanetskii, M. D.; Egholm, M.; Buchardt, O.; Sönnichsen, S. H.; Nielsen, P. E. *Biochem. Pharmacol.* **1994**, *48*, 1310−1313.
(9) Wittung, P.; Nielsen, P. E.; Nordén, B. *J. Am. Chem. Soc.* **1996**, *118*, 7049−7054.
(10) Lohse, J.; Dahl, O.; Nielsen, P. E. *Proc. Natl. Acad. Sci. U.S.A.* **1999**, *96*, 11804−11808.
(11) Ishihara, T.; Corey, D. R. *J. Am. Chem. Soc.* **1999**, *121*, 2012−2020.
(12) Zhang, X.; Ishihara, T.; Corey, D. R. *Nucleic Acids Res.* **2000**, *28*, 3332−3338.
(13) Larsen, H. J.; Nielsen, P. E. *Nucleic Acids Res.* **1996**, *24*, 458−463.
(14) Hanvey, J. C.; Peffer, N. J.; Bisi, J. E.; Thomson, S. A.; Cadilla, R.; Josey, J. A.; Ricca, D. J.; Hassman, C. F.; Bonham, M. A.; Au, K. G.; Carter, S. G.; Bruckenstein, D. A.; Boyd, A. L.; Noble, S. A.; Babiss, L. E. *Science* **1992**, *258*, 1481−1485.
(15) Knudsen, H.; Nielsen, P. E. *Nucleic Acids Res.* **1996**, *24*, 494−500.
(16) Good, L.; Nielsen, P. E. *Proc. Natl. Acad. Sci. U.S.A.* **1998**, *95*, 2073−2076.
(17) Good, L.; Nielsen, P. E. *Nature Biotechnol.* **1998**, *16*, 355−358.
(18) Good, L.; Awasthi, S. K.; Dryselius, R.; Larsson, O.; Nielsen, P. E. *Nature Biotechnol.* **2001**, *19*, 360−364.
(19) Greider, C. W. *Annu. Rev. Biochem.* **1996**, *65*, 337.
(20) Kim, N. W.; Piatyszek, M. A.; Prowse, K. R.; Harley, C. B.; West, M. D.; Ho, P. L. C.; Coviello, G. M.; Wright, W. E.; Weinrich, S. L.; Shay, J. W. *Science* **1994**, *266*, 2011.

10.1021/ja016204c CCC: $20.00
Published on Web 09/08/2001

telomerase and inhibiting the enzyme.[22−28] PNA has also been used for detection and sizing of telomeric DNA.[29−31] These studies are significant especially due to the close association between telomere length and expected life span for some cell lines, an association which forms the basis for the telomere hypothesis of aging.[32]

The antisense strategy appears straightforward based on simply reading the sequence of the RNA target and synthesizing a complementary probe. However, a recent study by Corey and co-workers revealed that the only PNAs that successfully blocked translation of a particular mRNA were those targeted to the 5′-untranslated region.[33] Likewise, PNAs that were targeted to the active site of telomerase effectively inhibited the enzyme, but shifting the target sequence away from the active site by even one nucleotide led to virtually complete loss of activity.[23] These results raise the question of how the secondary and tertiary structures in the target affect hybridization by the PNA. To begin defining the scope of applicability for PNA antisense/antigene reagents, we initiated work aimed at determining the ability of short PNA oligomers to overcome secondary structure in folded DNA and RNA targets. As an initial test system, we selected as a target the DNA quadruplex motif, which arises from the stacking of hydrogen-bonded G-tetrads.[34] Relatively short DNA sequences are known to fold into stable, intramolecular quadruplex structures.[34] It may be noted that telomeres have long been postulated to form G-quadruplexes similar to triplet repeat DNAs.[35] While there is no conclusive evidence of telomeric quadruplexes being present in vivo, a number of in vitro studies clearly support the possibility, although a recent report indicates that such structures may not be formed in mammalian cells.[36] We now report that a short 7-mer PNA probe complementary to the central seven bases of a G-quadruplex spontaneously disrupts the target secondary structure and forms a surprisingly stable PNA−DNA hybrid duplex. The source of this stability is attributed to overhanging bases from the DNA strand, an effect that is not observed for an analogous DNA probe.

Experimental Section

Materials. PNA oligomers were synthesized using standard solid-phase synthesis protocols.[37,38] Boc/Z-protected PNA monomers were purchased from Perseptive Biosystems (Framingham, MA). Boc-protected Lys-MBHA resin was used, and the synthesis was performed on a 100 mg scale. Oligomers were purified using reversed-phase HPLC and characterized by MALDI-TOF spectrometry (P1, calculated mass 1954.01, observed mass 1951.45; P2, calculated mass 1824.83, observed mass 1824.83). PNA P3 was a gift from Stuart Kushon. Stock solutions of the PNA were prepared in 10 mM sodium phosphate buffer (pH 7.0). The absorbance values used for calculating concentrations were measured after incubating at 50 °C to disrupt the PNA secondary structure.[39] DNA oligomers were purchased from Integrated DNA Technologies, Inc. (Coralville, IA). In one case, the DNA was purified by HPLC, but the experimental results were indistinguishable from those for material purified by simple gel filtration (GF). Thus, the less expensive GF grade DNA was used for all other experiments. Concentrations were determined spectrophotometrically using the absorbance at 260 nm, and the extinction coefficients were calculated using the Schepartz Lab Biopolymer Calculator (http://paris.chem.yale.edu/extinct.html). The cyanine dye $DiSC_2(5)$ was purchased from Molecular Probes, Inc. (Eugene, OR) and used without further purification. (This dye is no longer available from Molecular Probes but can be purchased from Aldrich Chemical Co., Milwaukee, WI.) Stock solutions were prepared in methanol, and concentrations were determined using the manufacturer's extinction coefficient (ϵ_{651} = 260 000 M^{-1} cm^{-1}).

Equipment. UV−vis measurements were performed on a Varian Cary 3 spectrophotometer equipped with a thermoelectrically controlled multicell holder. Circular dichroism (CD) spectra were recorded on a Jasco J-715 spectropolarimeter equipped with a thermoelectrically controlled single cell holder.

Hybridization. PNA or DNA hybridization with the quadruplex was monitored by CD. PNA or DNA probes were added to the quadruplex (5 μM each) in a buffer containing 10 mM potassium phosphate (pH 7.2) and 10 or 250 mM KCl at 37 °C and then allowed to stand for 5 min at the same temperature before recording of spectra. Spectra shown represent the average of eight scans recorded at 100 nm/min.

Cyanine Dye Titration. A PNA−DNA hybrid was prepared as described above, with 10% methanol and 10 mM KCl included in the buffer. $DiSC_2(5)$ was then added in 2.0 μM increments. CD spectra were acquired from 750 to 450 nm after each addition.

Continuous Variations Experiment. Samples containing variable amounts of PNA and DNA (total concentration, 10 μM) were prepared in 10 mM potassium phosphate and 10 mM KCl. CD spectra were recorded at 37 °C after equilibration for 5 min, and the CD signal at 294 nm was plotted versus the mole fraction of PNA.

Thermal Analysis. Unless otherwise indicated, samples were heated to 90 °C (UV−vis and CD experiments) and equilibrated for 5 min. UV−vis absorbance at 272 nm and CD intensity at 294 nm were recorded every 0.5 °C as samples were cooled and then heated at a rate of 1.0 °C/min. (Experiments performed at 0.5 °C/min yielded identical results.) No hysteresis was observed in the transitions detected for any of the quadruplexes or duplexes. Experiments were done in triplicate; the values given in the data tables reflect the averages of those measurements. Thermodynamic parameters were determined from curve-fitting data from heating ramps.

Results

Target Selection. The 15-base DNA sequence TBA shown in Chart 1 was isolated from an in vitro selection experiment on the basis of its affinity for the protein thrombin.[40] This sequence, given the name "thrombin binding aptamer" or TBA,

(21) Salazar, M.; Thompson, B. D.; Kerwin, S. N.; Hurley, L. H. *Biochemistry* **1996**, *35*, 16110.
(22) Norton, J. C.; Piatyszek, M. A.; Wright, W. E.; Shay, J. W.; Corey, D. R. *Nature Biotechnol.* **1996**, *14*, 615−619.
(23) Hamilton, S. E.; Pitts, A. E.; Katipally, R. R.; Jia, X.; Rutter, J. P.; Davies, B. A.; Shay, J. W.; Wright, W. E.; Corey, D. R. *Biochemistry* **1997**, *36*, 11873−11880.
(24) Pitts, A. E.; Corey, D. R. *Proc. Natl. Acad. Sci. U.S.A.* **1998**, *95*, 11549−11554.
(25) Harrison, J. G.; Frier, C.; Laurant, R.; Dennis, R.; Raney, K. D.; Balasubramanian, S. *Bioorg. Med. Chem. Lett.* **1999**, *9*, 1273−1278.
(26) Hamilton, S. E.; Simmons, C. G.; Kathiriya, I. S.; Corey, D. R. *Chem. Biol.* **1999**, *6*, 343−351.
(27) Herbert, B.-S.; Pitts, A. E.; Baker, S. I.; Hamilton, S. E.; Wright, W. E.; Shay, J. W.; Corey, D. R. *Proc. Natl. Acad. Sci. U.S.A.* **1999**, *96*, 14276−14281.
(28) Villa, R.; Folini, M.; Lualdi, S.; Veronese, S.; Daidone, M. G.; Zaffaroni, N. *FEBS Lett.* **2000**, *473*, 241−248.
(29) Rufer, N.; Dragowska, W.; Thornbury, G.; Roosnek, E.; Lansdorp, P. M. *Nature Biotechnol.* **1998**, *16*, 743−747.
(30) Hultdin, M.; Grönlund, E.; Norrback, K.-F.; Erikkson-Lindström, E.; Just, T.; Roos, G. *Nucleic Acids Res.* **1998**, *26*, 3651−3656.
(31) Serakinci, N.; Koch, J. *Nature Biotechnol.* **1999**, *17*, 200−201.
(32) Bodnar, A. G.; Ouelette, M.; Frolkis, M.; Holt, S. E.; Chiu, C.-P.; Morin, G. B.; Harley, C. B.; Shay, J. W.; Lichtsteiner, S.; Wright, W. E. *Science* **1998**, *279*, 349.
(33) Doyle, D. F.; Braasch, D. A.; Simmons, C. G.; Janowski, B. A.; Corey, D. R. *Biochemistry* **2001**, *40*, 53−64.
(34) Williamson, J. R. *Annu. Rev. Biophys. Biomol. Struct.* **1994**, *23*, 703−730.
(35) Williamson, J. R.; Raghuraman, M. K.; Cech, T. R. *Cell* **1989**, *59*, 871−880.
(36) Griffith, J. D.; Comeau, L.; Rosenfield, S.; Stansel, R. M.; Bianchi, A.; Moss, H.; de Lange, T. *Cell* **1999**, *97*, 503−514.
(37) Christensen, L.; Fitzpatrick, R.; Gildea, B.; Petersen, K. H.; Hansen, H. F.; Koch, T.; Egholm, M.; Buchardt, O.; Nielsen, P. E.; Coull, J.; Berg, R. H. *J. Peptide Sci.* **1995**, *3*, 175−183.
(38) Koch, T.; Hansen, H. F.; Andersen, P.; Larsen, T.; Batz, H. G.; Otteson, K.; Ørum, H. *J. Peptide Res.* **1997**, *49*, 80−88.
(39) Ratilainen, T.; Holmén, A.; Tuite, E.; Haaima, G.; Christensen, L.; Nielsen, P. E.; Nordén, B. *Biochemistry* **1998**, *37*, 12331−12342.

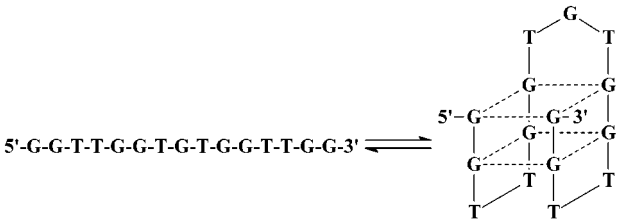

Figure 1. Primary structure and quadruplex secondary structure of thrombin binding aptamer (TBA) DNA. Solid and dashed lines indicate covalent and hydrogen bonding connections, respectively.

Chart 1. PNA and DNA Sequences Used

Name	Sequence
TBA	5'-GGTTGGTGTGGTTGG-3'
P1	H-CCACACC-Lys-NH_2
P2	H-CCACACC-NH_2
P3	H-CGTTTCCG-Lys-NH_2
Q	5'-GGTTGGTTTGGTTGG-3'
D1	5'-CCACACC-3'
7mer DNA	5'-GGTGTGG-3'

folds into a stable, intramolecular quadruplex structure featuring two stacked guanine tetrads and three loops (Figure 1).[41] We selected this as a potential target for PNA hybridization for two reasons. First, TBA represents a simple secondary structure to test the impact of target folding on probe hybridization. While target structure can be reasonably expected to block access of a probe to its complementary sequence, there has been very little quantitative analysis of the impact on the thermodynamics of hybridization. Second, there are numerous reports of PNA hybridization to telomeric DNA.[29−31] In particular, fluorescent PNAs have been used to determine the length of telomeres.[29−31] Telomeric DNA is guanine rich and may form intramolecular quadruplexes in vivo.[35] However, no experiments have been reported in which the ability of PNA to hybridize to quadruplex DNA has been directly demonstrated.

Characterization of TBA. The 15mer DNA target TBA was suspended in aqueous potassium phosphate buffer (10 mM, KPi, pH = 7.2, 10 mM KCl), incubated at 90 °C for 10 min, and then slowly cooled to 37 °C to promote folding into a quadruplex structure. This was necessary to maximize the CD signal. The circular dichroism (CD) spectrum of TBA (Figure 2) matches that reported in the literature, demonstrating that the quadruplex is formed. In particular, the signature bands for antiparallel quadruplexes were observed: a maximum between 285 and 295 nm and a minimum between 265 and 270 nm.[42]

Heating causes the quadruplex to undergo a cooperative transition with a "melting temperature" (T_m) of 46.7 °C (inset, Figure 2). Curve fitting according to the method of Marky and Breslauer[43] yielded the free energy, enthalpy, and entropy of formation shown in Table 1. We note that this method assumes that the melting of TBA is a two-state transition, and extrapolation of the thermodynamic parameters to 25 °C requires that the transition occur with no change in heat capacity (ΔC_p). First derivative curves for either UV or CD melting curves recorded for TBA show no evidence for multiple transitions, suggesting that the two-state model should hold for TBA. The latter assumption regarding the ΔC_p has been shown recently to be invalid for the melting of duplexes to single strands.[44] However, another study revealed that the intramolecular melting of an RNA hairpin occurred with a very small ΔC_p, and correcting for this change had a negligible effect on the derived thermodynamic parameters.[45] To determine whether melting of the TBA quadruplex occurred with a significant ΔC_p, we measured T_m curves at various KCl concentrations between 25 and 250 mM. The thermodynamic stability of the quadruplex is dependent on the ionic strength, resulting in a shift of the T_m to higher values as the KCl concentration increases. The ΔH at the T_m did not change within experimental error over a range of 8 °C variation in T_m (Figure S1). This indicates that there is little or no change in ΔC_p for melting of the TBA quadruplex, justifying the use of curve fitting to extract thermodynamic parameters.

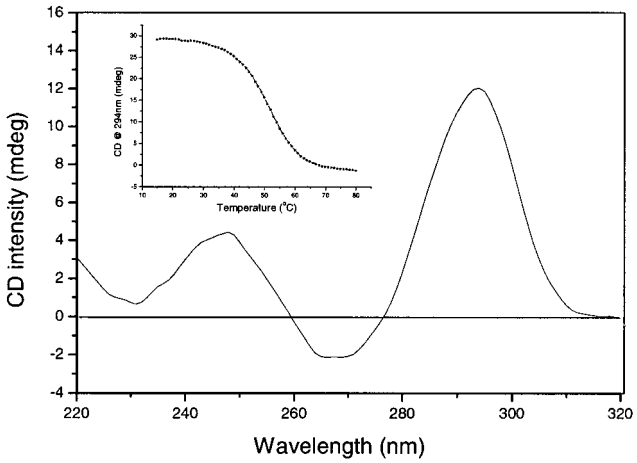

Figure 2. CD spectrum of 5 μM TBA at 37 °C in 10 mM KCl, 10 mM KPi buffer, pH 7.2. Inset shows the CD melting profile of TBA. CD was monitored at 294 nm.

Table 1. Melting Temperatures and Thermodynamic Parameters for DNA Target and PNA−DNA Hybrids (Thermodynamic Parameters Given in kcal/mol)

structure	T_m (°C)	ΔG_{298}	ΔH	$T\Delta S$
TBA quadruplex[a]	46.7 ± 0.2	−2.8 ± 0.2	−40.0 ± 0.5	−37.2 ± 0.4
TBA/P1 hybrid	55.2 ± 0.2	−11.7 ± 0.1	−43.9 ± 1.3	−32.2 ± 1.2
5′-GGTGTGG-3′/ P1 hybrid	36.1 ± 0.1	−9.4 ± 0.1	−47.7 ± 0.6	−38.4 ± 0.3

[a] Thermodynamic parameters calculated from CD spectra.

Hybridization of P1 with TBA. To study PNA hybridization with TBA, a seven-base region of the latter was chosen as the target. This region was selected so as to include both the stem (i.e., tetrads) and TGT loop, regions that are critical to the stability of the quadruplex (Scheme 1). The complementary PNA P1 (Chart 1) was synthesized using standard solid-phase peptide synthesis protocols.[37,38] Three experiments were performed to characterize the interaction of P1 with TBA. First, circular dichroism spectra were recorded for TBA alone, P1 alone, and a 1:1 mixture of the two (Figure 3). The spectrum of the mixture is not simply the sum of the individual components, demonstrating interaction between the two strands. Moreover, the extrema

(40) Bock, L. C.; Griffin, L. C.; Latham, J. A.; Vermaas, E. H.; Toole, J. J. *Nature* **1992**, *355*, 564−566.
(41) Wang, K. Y.; McCurdy, S.; Shea, R. G.; Swaminathan, S.; Bolton, P. H. *Biochemistry* **1993**, *32*, 1899−1904.
(42) Williamson, J. R. *Curr. Opin. Struct. Biol.* **1993**, *3*, 357.
(43) Marky, L. A.; Breslauer, K. J. *Biopolymers* **1987**, *26*, 1601−1620.
(44) Chalikian, T. V.; Völker, J.; Plum, G. E.; Breslauer, K. J. *Proc. Natl. Acad. Sci. U.S.A.* **1999**, *96*, 7853−7858.
(45) Diamond, J. M.; Turner, D. H.; Mathews, D. H. *Biochemistry* **2001**, *40*, 6971−6981.

Scheme 1. Invasion of DNA Quadruplex TBA by P1

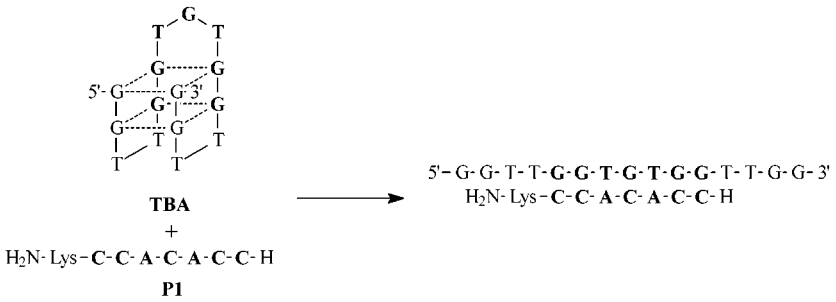

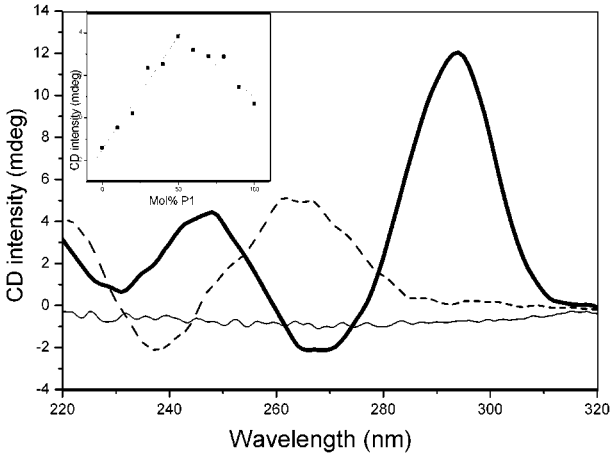

Figure 3. Comparative CD spectra of TBA alone (thick solid line), 1:1 mixture of P1 + TBA (5 μM each, dashed line), and P1 alone (thin solid line) in 10 mM KCl, 10 mM KPi buffer, pH 7.2. Inset shows Job plot for CD intensity of P1 + TBA at a total concentration of 10 μM at $\lambda = 272$ nm.

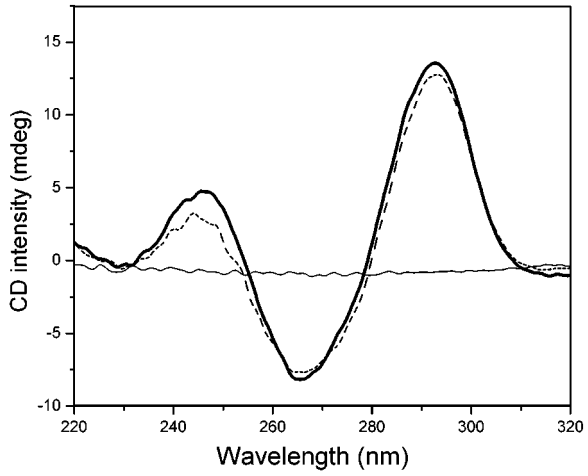

Figure 4. Comparative CD spectra of quadruplex Q alone (thick solid line), 1:1 mixture of Q + P1 (5 μM each, dashed line), and P1 alone (thin solid line) in 10 mM KCl, 10 mM KPi buffer, pH 7.2.

exhibited by the mixture, namely the maximum at 262 nm and the minimum at 238 nm, are typical of PNA−DNA duplexes in which the PNA N-terminus is aligned with the DNA 3′-terminus.[7] A continuous variations experiment demonstrates that the interaction between P1 and TBA yields a complex with 1:1 stoichiometry (Figure 3, inset). Moreover, a 1:1 mixture of P1 and the quadruplex Q (Chart 1) yielded a CD spectrum that was simply the sum of the individual components, indicating no interaction between the two strands (Figure 4). The sequence of Q features a TTT central loop in place of TGT for the TBA quadruplex, which introduces a mismatch at the central position

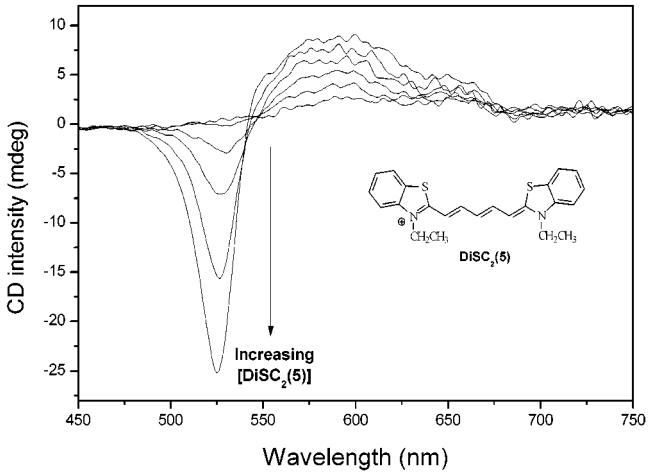

Figure 5. CD titration of $DiSC_2(5)$ (inset) into P1−TBA hybrid. Spectra were recorded at 37 °C in 10 mM KCl, 10 mM KPi buffer, pH 7.2, with 10% MeOH. TBA and P1 were 5 μM in strands and were not annealed prior to titration of dye. Dye was added in increments of 2 μM.

for hybridization of P1. Smirnov and Shafer previously showed that this sequence folds into the same quadruplex structure as TBA and has comparable thermodynamic stability.[46] The failure of P1 to hybridize to Q indicates that P1 and TBA bind sequence specifically to form a double-helical PNA−DNA hybrid stabilized by Watson−Crick base pairing.

In a second experiment, the cyanine dye $DiSC_2(5)$ (Figure 5) was added to the P1−TBA hybrid. We previously demonstrated high-affinity binding of this dye to PNA−DNA hybrids.[47] The dye binds as a helical aggregate and is readily detected as a blue−purple color change as well as distinct visible absorption and CD bands. Figure 5 illustrates the induced CD spectrum for $DiSC_2(5)$ in the presence of the P1−TBA hybrid. The exciton splitting of the CD band is consistent with a right-handed helical arrangement of the dye molecules within the aggregate as expected for a right-handed helical template, provided by the PNA−DNA duplex.

Finally, UV melting curves characterized the P1−TBA hybrid. These experiments were performed at 272 nm, which yields a substantially larger hyperchromicity upon denaturation than does the absorbance at 260 nm. Figure 6 illustrates a melting curve recorded for the P1−TBA hybrid. Curve fitting revealed a melting temperature of $T_m = 55.2$ °C, with thermodynamic values for the process given in Table 1.

Effect of DNA Overhangs on PNA−DNA Stability. The P1−DNA hybrid exhibited unexpectedly high thermal and thermodynamic stabilities for a seven-base-pair duplex. Other

(46) Smirnov, I.; Shafer, R. F. *Biochemistry* **2000**, *39*, 1462−1468.
(47) Smith, J. O.; Olson, D. A.; Armitage, B. A. *J. Am. Chem. Soc.* **1999**, *121*, 2686−2695.

Table 2. Effect of DNA Overhangs on Stability of P1−DNA Hybrid (Thermodynamic Parameters Given in kcal/mol)

DNA target	T_m (°C)	ΔG_{298}	ΔH	$T\Delta S$
5′-GGTGTGG-3′	36.1 ± 0.1	−9.4 ± 0.1	−47.7 ± 0.6	−38.4 ± 0.3
5′-**T**GGTGTGG**T**-3′	34.8 ± 0.2	−9.5 ± 0.1	−49.9 ± 1.8	−40.4 ± 1.9
5′-**TT**GGTGTGG**TT**-3′	46.5 ± 0.7	−11.1 ± 0.1	−51.6 ± 1.7	−40.5 ± 1.6
5′-**GTT**GGTGTGG**TTG**-3′	50.3 ± 0.3	−11.9 ± 0.1	−54.7 ± 0.5	−42.7 ± 0.4
5′-**GGTT**GGTGTGG**TTGG**-3′	55.2 ± 0.2	−11.7 ± 0.1	−43.9 ± 1.3	−32.2 ± 1.2
5′-**TGGTT**GGTGTGG**TTGGT**-3′	56.3 ± 0.2	−12.9 ± 0.4	−55.9 ± 4.2	−43.0 ± 4.3

Table 3. Effect of DNA Overhang Sequence on Stability of P1−DNA Hybrid (Thermodynamic Parameters Given in kcal/mol)

DNA target	T_m (°C)	ΔG	ΔH	$T\Delta S$
5′-**ATTA**GGTGTGG**ATTA**-3′	54.0 ± 0.1	−12.7 ± 0.1	−56.5 ± 0.5	−43.8 ± 0.3
5′-**ATTG**GGTGTGG**GTTA**-3′	54.3 ± 0.6	−12.7 ± 0.2	−57.8 ± 1.6	−45.1 ± 1.4
5′-**ATTC**GGTGTGG**CTTA**-3′	56.4 ± 0.2	−13.5 ± 0.3	−63.5 ± 2.2	−50.0 ± 1.9
5′-**ATT*T***GGTGTGG***T***TTA**-3′	51.9 ± 0.6	−12.5 ± 0.2	−57.9 ± 2.4	−45.4 ± 2.2

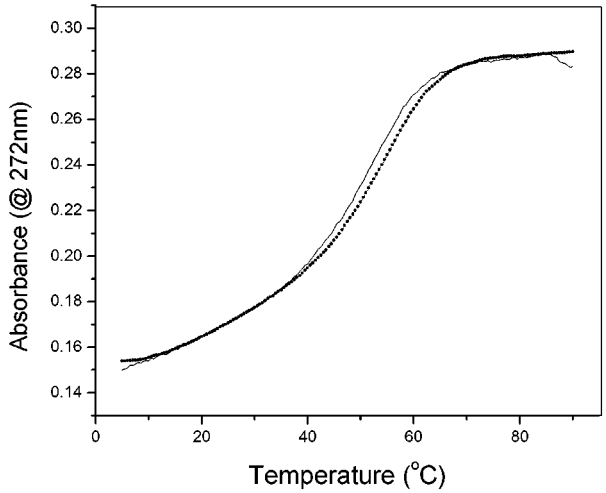

Figure 6. UV−vis melting profile of P1−TBA hybrid at 10 mM KCl, 10 mM KPi buffer, pH 7.2, at 5 μM of strands. Cooling ramp (solid line) and heating ramp (dotted line) were recorded at $\lambda = 272$ nm at the rate of 1 °C/min.

PNA−DNA hybrids exhibit anomalously high stability,[23] but those sequences typically possess three consecutive G−C base pairs whereas in P1−TBA, only two consecutive G−C pairs are present (at each end of the hybrid). To examine whether the stability was simply due to the sequence, we compared hybridization of P1 with TBA and the 7mer DNA complement, 5′-GGTGTGG-3′. The two hybrids exhibit similar CD spectra (Figure S2); however, the blunt-ended duplex formed with the 7mer DNA denatured at $T_m = 36.1$ °C, i.e., 19 °C lower than that for the P1−TBA. The two hybrids should contain the same number of Watson−Crick base pairs ordered in the same sequence, but the thermal stability is much higher when there are overhanging bases on the DNA strand flanking the duplex. This enhanced thermal stability also carries over into thermodynamic stability, as the P1−TBA hybrid is more stable by 2.3 kcal/mol than the P1−7mer complement hybrid (Table 1).

The origin of this effect was initially probed by varying the length of the overhangs. Table 2 provides T_m and thermodynamic data for six sequences representing four truncations and one extension of TBA, plus TBA itself. The results illustrate that single thymine overhangs on each end have a minimal effect, but overhangs of two, three, and five nucleotides stabilize the hybrid by 1.7, 2.5, and 3.5 kcal/mol, respectively. The lower stabilization for the four-base overhangs is due to the folded quadruplex structure formed by this sequence (vide infra). Based on CD analysis (Figure S3), the sequence having five overhanging nucleotides also folds into a quadruplex structure, but this quadruplex melts 15 °C lower than TBA and, therefore, presents a much lower thermodynamic barrier to hybridization.

Another issue to consider is whether the enhanced stability is dependent on the sequences of the overhangs. Table 3 provides thermal and thermodynamic data for hybrids in which the overhangs were 5′-ATT*X*-3′/5′-*X*TTA-3′ rather than 5′-GGTT-3′/5′-TTGG-3′, as with TBA. For ATTA overhangs, the T_m value was essentially identical to that for TBA, and the ΔG was 1.0 kcal/mol more favorable. In addition, significant stabilizations arise regardless of the identity of the first base in the overhang (Table 3). Interestingly, the hybrid with a C in the first overhanging position was found to be more stable than either G or T. These results clearly show that the overhang effect is not specific to the sequence of overhanging bases on the P1−TBA hybrid.

We next considered the possibility that overhang stabilization is unique to the P1 sequence. PNA P3 (Chart 1), having an eight-base sequence that is completely different from P1, was hybridized with the targets shown in Table 4. The thermal and thermodynamic stabilizations are evident. Even eight-base overhangs on the two ends of the hybrid yield substantial stabilization relative to a blunt-ended duplex, indicating that the influence of unpaired nucleotides extends for considerable distances beyond the end of the hybrid. Moreover, this result shows that the overhang effect is not specific to the P1 sequence.

Finally, we analyzed sequences that contained only one overhang, on either end of the hybrid (Table 5). The data clearly show that 3′-overhangs contribute more to the stabilization than do 5′-overhangs, although the latter are stabilizing in their own right. In the antiparallel orientation favored by PNA, the N-terminus is aligned with the 3′-end of the DNA. This places the C-terminal lysine residue at the 5′-end of the DNA. To ascertain whether the lysine residue was interacting unfavorably with the 5′-overhang and, therefore, reducing the amount of stabilization relative to the 3′-overhang, we synthesized PNA P2, which has the same sequence as P1 but lacks the C-terminal lysine. The data in Table 6 illustrate the electrostatic importance of the lysine residue, since the ΔG and T_m values are less favorable than they were for P1. However, the decreases in stability are slightly greater with the 5′-overhang than with the 3′-overhang, indicating that the lysine residue in P1 actually stabilizes the former.

Comparison of PNA and DNA Hybridization Probes. PNA typically exhibits substantially higher affinity for complementary DNA or RNA targets than does a corresponding DNA probe.[7] This effect is also observed when targeting the TBA quadruplex. Thus, the CD spectrum for a 1:1 mixture of TBA and D1 (5′-CCACACC-3′) was simply the sum of the spectra for the two

Table 4. Effect of DNA Overhangs on P3-DNA Hybrids (Thermodynamic Parameters Given in kcal/mol)

overhangs	T_m (°C)	ΔG_{298}	ΔH	$T\Delta S$
none	35.7 ± 0.6	−9.6 ± 0.1	−54.6 ± 0.9	−45.0 ± 0.9
5′-ATTA-3′/ 5′-ATTA-3′	49.0 ± 0.1	−11.7 ± 0.1	−58.0 ± 1.3	−46.3 ± 1.2
5′-TATTATTA-3′/ 5′-ATTATTAT′3′	58.0 ± 0.8	−13.8 ± 0.7	−61.6 ± 4.5	−47.8 ± 4.5

Table 5. Effect of Overhang Position on P1−DNA Hybrid Stability (Thermodynamic Parameters Given in kcal/mol)

DNA target	T_m (°C)	ΔG_{298}	ΔH	$T\Delta S$
5′-GGTGTGG-3′	36.1 ± 0.1	−9.4 ± 0.1	−47.7 ± 0.6	−38.4 ± 0.3
5′-**ATTA**GGTGTGG-3′	44.0 ± 0.1	−10.9 ± 0.1	−55.2 ± 2.1	−44.3 ± 2.0
5′-GGTGTGG**ATTA**-3′	48.4 ± 0.3	−11.7 ± 0.1	−57.1 ± 2.1	−45.4 ± 2.1
5′-**ATTA**GGTGTGG**ATTA**-3′	54.0 ± 0.1	−12.7 ± 0.1	−56.5 ± 0.5	−43.8 ± 0.3

Table 6. Effect of Overhang Position on P2−DNA Hybrid Stability (Thermodynamic Parameters Given in kcal/mol)

DNA target	T_m (°C)	ΔG_{298}	ΔH	$T\Delta S$
5′-GGTGTGG-3′	32.7 ± 0.2	−8.9 ± 0.2	−47.3 ± 0.6	−38.3 ± 0.6
5′-**ATTA**GGTGTGG-3′	38.3 ± 0.6	−9.7 ± 0.1	−49.8 ± 0.5	−40.2 ± 0.4
5′-GGTGTGG**ATTA**-3′	44.0 ± 0.1	−10.7 ± 0.1	−52.4 ± 1.4	−41.7 ± 1.4
5′-**ATTA**GGTGTGG**ATTA**-3′	49.4 ± 0.6	−11.3 ± 0.4	−52.2 ± 4.2	−40.9 ± 3.9

Table 7. Effect of Overhang Position on D1−DNA Hybrid Stability (Thermodynamic Parameters Given in kcal/mol)

DNA target	T_m (°C)	ΔG_{298}	ΔH	$T\Delta S$
5′-GGTGTGG-3′	32.7 ± 0.5	−8.7 ± 0.2	−48.3 ± 0.1	−39.5 ± 0.2
5′-**ATTA**GGTGTGG-3′	35.0 ± 0.7	−9.3 ± 0.1	−51.4 ± 0.6	−42.1 ± 0.5
5′-GGTGTGG**ATTA**-3′	29.1 ± 0.4	−8.1 ± 0.1	−50.2 ± 3.5	−42.1 ± 3.5
5′-**ATTA**GGTGTGG**ATTA**-3′	32.6 ± 0.6	−8.8 ± 0.1	−51.2 ± 2.8	−42.4 ± 2.8
5′-**GGTT**GGTGTGG-3′	34.4 ± 0.5	−9.1 ± 0.1	−52.6 ± 4.0	−43.5 ± 3.9
5′-GGTGTGG**TTGG**-3′	29.0 ± 0.6	−8.2 ± 0.1	−47.1 ± 1.4	−38.9 ± 1.4
5′-**GGTT**GGTGTGG**TTGG**-3′[a]	−	−	−	−

[a] No hybridization detected at 250 mM KCl.

individual components, reflecting no interaction between the two strands at 37 °C (Figure S4, inset). However, a melting curve for the mixture did show two transitions: one at 12 °C, which we assign to the TBA−D1 hybrid, and the other at 47 °C, due to TBA unfolding (Figure S5). Thus, the T_m for the hybrid formed by quadruplex invasion by the DNA probe was 43 °C lower than that for the corresponding PNA probe.

We next attempted to analyze the overhang effect in the context of DNA−DNA duplexes. Formation of stable duplexes required increasing the KCl concentration to 100 mM. Table 7 contains data for the effect of two different overhangs on hybridization of D1 with the 5′-GGTGTGG-3′ target. In both cases, the 5′-overhang stabilizes the hybrid, while the 3′-overhang destabilizes it.[48] The net effect, in the case of the ATTA overhangs, is no stabilization relative to the blunt-ended duplex. For the GGTT/TTGG overhangs, no hybridization by the DNA probe is observed, although this is likely due to the increase in stability of the TBA secondary structure at 100 mM KCl rather than to the impact of the overhangs on the D1−TBA hybrid.

Effect of DNA Structure on PNA Hybridization. The TBA target is quite different from other DNA sequences used to study PNA hybridization because it possesses a folded secondary structure. However, the P1−TBA hybrid denatures at 55.2 °C in the low salt buffer used for most experiments. This is 8.7 °C higher than the denaturation temperature for the TBA quadruplex. Thus, when the P1−TBA hybrid melts, the DNA strand cannot refold into the quadruplex structure. If the KCl concentration is increased from 10 to 250 mM, the TBA quadruplex T_m rises to 55.5 °C, while the P1−TBA T_m decreases to 33.7 °C. Under these conditions, the P1−TBA hybrid melts at a temperature that allows the DNA strand to refold into the quadruplex secondary structure (Scheme 2). This has a significant impact on the thermodynamics of denaturation. Table 8 illustrates this by comparing P1 hybridization to TBA and to the analogous unstructured sequence that has only three-base overhangs. (The DNA with three-base overhangs did not give the characteristic antiparallel quadruplex CD spectrum, Figure S6.) The results reveal that the hybrid formed with the unstructured target is destabilized at the higher salt concentration: $\Delta T_m = -9.4$ °C and $\Delta\Delta G = 1.9$ kcal/mol, but this is far less than the structured TBA target: $\Delta T_m = -21.5$ °C and $\Delta\Delta G = 3.4$ kcal/mol.

Discussion

Quadruplex Invasion. The present study is the first example of a PNA probe hybridizing to a folded DNA quadruplex. While strand invasion of PNA into duplex DNA has been studied in detail, less attention has been paid to the ability of PNA to disrupt secondary structures of DNA such as hairpins, quadruplexes, and cruciforms. In parallel work, we are studying the ability of PNA to disrupt the extremely stable class of GNRA DNA hairpins.[49] The present studies focused on an alternative

(48) Preferential stabilization of DNA−DNA duplexes by 5′-overhangs has been reported for other systems: (a) Bommarito, S.; Peyret, N.; SantaLucia, J., Jr. *Nucleic Acids Res.* **2000**, *28*, 1929−1934. (b) Doktycz, M. J.; Paner, T. M.; Amaratunga, M.; Benight, A. S. *Biopolymers* **1990**, *30*, 829−845. (c) Marotta, S. P.; Sheardy, R. D. *Biophys. J.* **1996**, *71*, 3361−3369. (d) Senior, M.; Jones, R. A.; Breslauer, K. J. *Biochemistry* **1988**, *27*, 3879.

(49) Kushon, S. A.; Jordan, J. P.; Seifert, J. L.; Nielsen, P. E.; Nielsen, H.; Armitage, B. A., manuscript submitted to *J. Am. Chem. Soc.* In press.

Scheme 2. Effect of Ionic Strength on Thermal Denaturation Pathway of TBA-P1 Hybrid

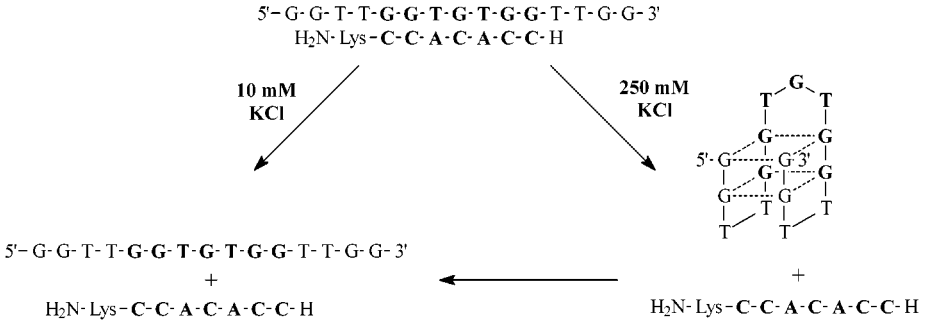

Table 8. Effect of Ionic Strength on P1−DNA Hybrid Stability (Thermodynamic Parameters Given in kcal/mol)

overhangs	[KCl] (mM)	T_m (°C)	ΔG_{298}	ΔH	$T\Delta S$
5′-GTT-3′/5′-TTG-3′	10	50.3 ± 0.2	−12.2 ± 0.2	−54.5 ± 0.8	−42.3 ± 0.7
5′-GTT-3′/5′-TTG-3′	250	40.9 ± 0.2	−10.3 ± 0.1	−50.5 ± 1.8	−40.2 ± 1.8
5′-GGTT-3′/5′-TTGG-3′	10	55.2 ± 0.2	−11.7 ± 0.1	−43.9 ± 1.3	−32.2 ± 1.2
5′-GGTT-3′/5′-TTGG-3′	250	33.7 ± 1.5	−8.3 ± 0.1	−24.0 ± 0.9	−15.7 ± 0.7

secondary structure, the guanine quadruplex. CD spectra (Figure 3) and an organic dye indicator (Figure 5) revealed successful hybridization of a PNA probe to the TBA quadruplex, while the sequence specificity of P1 in hybridizing to TBA was confirmed by the lack of interaction between P1 and the single mismatch quadruplex Q (Figure 4). Thus, a PNA seven-base probe successfully disrupts a stable DNA quadruplex to form a PNA−DNA hybrid at 37 °C. Under identical conditions, the corresponding DNA probe failed to hybridize, consistent with the higher affinity typically exhibited by PNA relative to DNA.

The secondary structure in the DNA target manifests in widely disparate thermodynamic parameters for hybridization of P1 in 10 and 250 mM KCl (Table 8). The differences in ΔG, ΔH, and ΔS at the two KCl concentrations arise from inversion of the relative stabilities of the TBA quadruplex and P1−TBA hybrid. Specifically, at the lower ionic strength, the P1−TBA hybrid denatures at a higher temperature (55.2 °C) than the TBA quadruplex (46.7 °C). Thus, once dissociated, the DNA strand cannot refold into the quadruplex structure (Scheme 2). However, at the higher ionic strength, the quadruplex denatures at a significantly higher temperature (55.5 °C). In this case, denaturation of the P1−TBA hybrid occurs at a temperature where refolding of the DNA strand can occur (Scheme 2). This is reflected in the thermodynamics for the two cases: ΔH for the P1−TBA hybrid decreases from −43.9 kcal/mol at 10 mM KCl to −24.0 kcal/mol at 250 mM KCl. The variation of the salt concentration is not expected to lower the Van't Hoff enthalpy to this extent.[50] However, $T\Delta S$ also becomes less negative at the higher ionic strength (−15.7 versus −32.2 kcal/mol). We propose that the significantly less negative enthalpy and entropy changes for PNA hybridization at the higher ionic strength reflect refolding of the dissociated DNA strand upon melting of the hybrid. Since the TBA structure is stabilized by intramolecular hydrogen bonding and stacking interactions, the enthalpy change is less than in the case of dissociation to unstructured single strands. Likewise, the folded TBA has far fewer conformational degrees of freedom than the unstructured DNA, decreasing the difference in entropy between the hybrid and the dissociated components at the T_m.

Previous work demonstrated PNA−DNA stability to be independent of ionic strength within physiological range.[50] However, the influence of ionic strength on the stability of target secondary/tertiary structure could significantly affect hybridization. In fact, the well-documented requirement for low ionic strength to permit strand invasion of PNA into duplex DNA targets is consistent with this.[9,51] Comparison of the Gibbs free energies of the hybrid at the two salt concentrations illuminates this phenomenon: at 10 mM KCl the ΔG for P1−TBA is −11.7 kcal/mol, while at 250 mM KCl it is −8.3 kcal/mol. The 3.4 kcal/mol decrease in driving force is due not to a decrease in the stability of the hybrid but rather to an increase in the stability of the TBA.

Overall, these experiments establish PNA as a quadruplex-disrupting agent. The ability of PNA to overcome a stable nonduplex DNA secondary structure and hybridize to its target sequence furthers the prospect of using PNA as an antigene reagent and probe.

The Overhang Effect. The significantly higher thermal and thermodynamic stabilities of the P1−TBA hybrid as compared to those of the analogous blunt-ended duplex call for closer inspection of the role of nonbonded overhanging nucleobases in PNA−DNA hybrids. If generalizable, this feature could significantly enhance the utility of PNA-based hybridization probes, since virtually all biological target sequences will result in overhangs on either end of the hybridized PNA. While the factors contributing to the thermodynamic stability of DNA double helices have been examined in detail,[52−54] similar studies on PNA−DNA duplexes have been limited to the contributions of hydrogen-bonding interactions and ionic strength effects.[39,55] Overhanging natural[48,57] and synthetic[56] nucleobases afford stabilization of DNA−DNA duplexes in some but not all cases. In addition, none of these experiments study systems where both 5′- and 3′-overhangs are present on the target strand, which is a more realistic representation of any hybridization process

(50) Tomac, S.; Sarkar, M.; Ratilainen, T.; Wittung, P.; Nielsen, P. E.; Nordén, B.; Gräslund, A. *J. Am. Chem. Soc.* **1996**, *118*, 5544−5552.

(51) Peffer, N. J.; Hanvey, J. C.; Bisi, J. E.; Thomson, S. A.; Hassman, C. F.; Noble, S. A.; Babiss, L. E. *Proc. Natl. Acad. Sci. U.S.A.* **1993**, *90*, 10648−10652.

(52) Gould, I. R.; Kollman, P. R. *J. Am. Chem. Soc.* **1994**, *116*, 2493.

(53) SantaLucia, J., Jr.; Allawi, H. T.; Seneviratne, P. A. *Biochemistry* **1996**, *35*, 3555.

(54) Bommarito, S.; Peyret, N.; SantaLucia, J. Jr. *Nucleic Acids Res.* **2000**, *28*, 1929−1934.

(55) Ratilainen, T.; Holmén, A.; Tuite, E.; Nielsen, P. E.; Nordén, B. *Biochemistry* **2000**, *39*, 7781−7791.

(56) Guckian, K. M.; Schweitzer, B. A.; Ren, R. X. F.; Sheils, C. J.; Tahmassebi, D. C.; Kool, E. T. *J. Am. Chem. Soc.* **2000**, *122*, 2213−2222.

(57) Senior, M.; Jones, R. A.; Breslauer, K. J. *Biochemistry* **1988**, *27*, 3879.

where the probe is significantly shorter than the target. Our experiments with D1 indicate that four-base overhangs offer no substantial stabilization within the sequence context of these hybrids. The generality of this phenomenon for PNA-containing hybrids is being explored in ongoing experiments in our laboratory, since it is possible that the effect will be attenuated for longer duplexes or other sequences. The point should still be made that because of the completely different chemical structures of the PNA and DNA backbones, significant differences in the factors that contribute to hybridization kinetics and thermodynamics will likely be uncovered by further experiments.

Lacking structural data regarding the overhanging bases, we can only speculate on the origin of this stabilization effect. PNA−DNA duplexes adopt different structures from $(DNA)_2$ duplexes.[58] Structurally, the eight-base-pair PNA−DNA duplex characterized by NMR is more loosely wound than B-form $(DNA)_2$ duplexes (13 bp/turn vs 10 bp/turn). This leads to a different stacking arrangement of the PNA−DNA nucleobases. Thus, even though PNA−DNA duplexes have a B-like conformation similar to $(DNA)_2$ duplexes, the existing structural differences could affect the ability of overhanging nucleobases to interact with the duplex terminus. In particular, better stacking of these bases with the less tightly wound PNA−DNA duplex may contribute to a more negative ΔH. A greater degree of stacking of the overhangs should also add to the entropic cost of hybridization, as reflected in the results in the data tables. Partially compensating enthalpy and entropy changes are known for DNA melting thermodynamics.[59] Hence, though we do not wish to overinterpret the present data, to illustrate our understanding of the overhang effect we can compare the ΔH and ΔS for the blunt-ended duplex with the P1−DNA hybrid with 5′-ATTA-3′ overhangs ($\Delta\Delta G = -3.6$ kcal/mol). For this hybrid, $\Delta\Delta H$ is −8.8 kcal/mol, while $T\Delta\Delta S$ is −5.2 kcal/mol (Table 2). In other words, the enthalpic gain is greater than the entropic penalty: the stabilization of the PNA−DNA hybrids due to overhangs on the DNA strand is evidently an enthalpic effect.

To determine whether the overhang effect was specific for the PNA−DNA sequence in the P1−TBA hybrid, the P3−DNA hybrids were studied (Table 4). The results presented in Table 4 indicate that the overhang effect extends for considerable length beyond the first few bases. Notably, addition of an eight-base overhang on either side increases the $\Delta\Delta G$ for the hybrid by −2.1 kcal/mol, beyond the −2.1 kcal/mol increase brought by the four-base overhang. Apparently the longer overhangs do not impose a substantial entropic penalty for the enthalpy to compensate. In addition, the increased thermal/thermodynamic stabilities of the P3−DNA hybrids are indicative of the overhang effect not being unique to the P1−TBA hybrid sequence.

The lack of an overhang effect for the corresponding DNA−DNA duplexes studied could arise from differences in the helical structure and/or electrostatics. Interestingly, the overhangs actually destabilize the D1−TBA hybrid relative to the blunt ended duplex ($\Delta T_m = -21.0$ °C), in contrast to the stabilization offered to P1 ($\Delta T_m = 19.0$ °C). In the former case, the stability of the TBA secondary structure suppresses the T_m for the D1−TBA hybrid, while in the case of the PNA probe, the overhang effect compensates for the target secondary structure, leading to facile quadruplex invasion.

Conclusion/Future Work. It is unknown at this time whether the overhang effect is unique to PNA or can be extended to other synthetic oligomers such as locked nucleic acid (LNA[60−62]). Furthermore, contribution of overhangs to stabilization of PNA−RNA hybrids could have an impact on antisense applications of PNA. Since nearest-neighbor interactions contribute significantly to nucleic acid hybridization thermodynamics, we are exploring the dependence of the overhang effect on the closing base pair of the duplex. Whether overhangs stabilize PNA−DNA/RNA hybrids when the target strand is hundreds or thousands of bases long also needs to be determined. Regardless of the answers to these questions, the experiments described above demonstrate that relatively short PNA probes can disrupt a folded quadruplex structure in target DNA sequences and form hybrids that are stabilized by overhanging nucleotides on the target strand.

Acknowledgment. We are grateful to the National Institutes of Health for financial support of this research (Grant R01GM58547-1A1). Mass spectra were measured in the Center for Molecular Analysis at Carnegie Mellon University, supported by NSF CHE-9808188. We thank Gabriel McMurtry for technical assistance and Stuart Kushon for helpful discussions and a sample of PNA P3. We also thank Prof. Gordon Rule for helpful discussions.

Supporting Information Available: CD spectra of P1−TBA, P1−7mer complement, and D1−TBA, melting curves for D1−TBA and D1−7mer complement, and a plot of ΔH vs T_m for TBA. This material is available free of charge via the Internet at http://pubs.acs.org.

JA016204C

(58) Erikkson, M.; Nielsen, P. E. *Nature Struct. Biol.* **1996**, *3*, 410−413.

(59) Petruska, J.; Goodman, M. F. *J. Biol. Chem.* **1995**, *270*, 746.

(60) Koshkin, A. A.; Singh, S. K.; Nielsen, P.; Rajwanshi, V. K.; Kumar, R.; Meldgaard, M.; Olsen, C. E.; Wengel, J. *Tetrahedron* **1998**, *54*, 3607−3630.

(61) Singh, S. K.; Wengel, J. *Chem. Commun.* **1998**, 1247−1248.

(62) Singh, S. K.; Nielsen, P.; Koshkin, A. A.; Wengel, J. *Chem. Commun.* **1998**, 455−456.